metals

MDPI

Review

Roles of Lanthanum and Cerium in Grain Refinement of Steels during Solidification

Yunping Ji [1,2], Ming-Xing Zhang [3] and Huiping Ren [1,2,*]

1 School of Material and Metallurgy, Inner Mongolia University of Science and Technology, Baotou 014010, China; jiyunpingpp@163.com
2 School of Materials Science and Engineering, Shanghai University, Shanghai 200072, China
3 School of Mechanical and Mining Engineering, The University of Queensland, Brisbane, QLD 4072, Australia; Mingxing.Zhang@uq.edu.au
* Correspondence: renhuiping@sina.com; Tel.: +86-472-595-2289; Fax: +86-472-595-4368

Received: 15 October 2018; Accepted: 25 October 2018; Published: 30 October 2018

Abstract: Refinement of as-cast structures is one of the most effective approaches to improve mechanical properties, formability, and surface quality of steel castings and ingots. In the past few decades, addition of rare earths (REs), lanthanum and cerium in particular, has been considered as a practical and effective method to refine the as-cast steels. However, previous reports contained inconsistent, sometime even contradictory, results. This review summaries the major published results on investigation of the roles of lanthanum or/and cerium in various steels, provides reviews on the similarity and difference of previous studies, and clarifies the inconsistent results. The proposed mechanisms of grain refinement by the addition of lanthanum or/and cerium are also reviewed. It is concluded that the grain refinement of steels by RE additions is attributed to either heterogeneous nucleation on the in-situ formed RE inclusions, a solute effect, or the combined effect of both. The models/theories for evaluation of heterogeneous nucleation potency and for solute effect on grain refinement of cast metals are also briefly summarized.

Keywords: lanthanum; cerium; steel; solidification; grain refinement; heterogeneous nucleation; solute role

1. Introduction

Generally, fine-grained microstructure leads to improved formability and to higher strength and toughness of steels. During solidification, microstructural refinement can also minimize the segregation and porosity in steel ingots or castings [1–4]. Hence, grain refinement has been regarded as an effective approach to improve the quality of steel products. Generally, grain refinement of steels can be achieved either by inoculation treatment of the steel melt to refine the as-cast microstructure or through refining austenite in the solid state. The former is termed as solidification grain refinement and the latter as solid grain refinement. The conventional solid grain refinement consists of adding strong carbide-forming elements, such as Nb, V, and Ti, during the steelmaking to enable carbides and carbonitride to precipitate during the subsequent hot working process, which impedes the growth of austenitic grains. The problem associated with this method is that the carbides or carbonitrides could reduce ductility by enabling surface transverse cracking during hot working if the process was not well-controlled [5]. Advanced solid grain refinement of steels is achieved through thermomechanical processing [6,7], which involves deforming and refining the supercooled austenite prior to transformation, and therefore the fine microstructure is obtained at room temperature. This thermomechanical processing, however, is not obviously suitable for cast steels. Furthermore, because the as-cast microstructure of steels has a direct influence on the subsequent formability of rolling or forging, and then on the mechanical properties of final steel products, control of the solidification is one of the key steps in controlling the quality of the final steel products.

Generally, the solidification grain refinement refers to minimization or elimination of columnar grains and refinement of the equiaxed grains. The currently available grain refinement techniques used during steel casting can be categorized as the following three groups:

• Electromagnetic stirring (EMS) [8,9]

This method is effective, but it has long-standing problems related to the mode of stirring, position of the stirrer, and stirring force [10]. In addition, the so called "white band" on a sulfur print of the stirred products, which is associated with negative segregation and positive segregation, is another critical issue [11]. Thus, EMS has limitations.

• Fast cooling [12,13]

This is another effective approach, but it is limited by the actual casting equipment and the actual size of the castings.

• Chemical grain refiners

Grain refinement is promoted through heterogeneous nucleation by the addition of a master alloy containing inoculant particles. This is commonly referred to as inoculation treatment and is considered to be the most cost-effective and practical technique to produce small equiaxed grains in a metal casting process [14,15]. Compared with cast aluminum alloys and cast magnesium alloys, in which the inoculation treatment is widely used in industrial practice, grain refinement is not the primary purpose of melt treatment during the steel making process, except for cast steels. However, in order to improve the quality of steels, researchers and engineers have realized its importance and have tried hard to identify effective grain refiners for steels, especially for cast steels [16–18], in the past few years. A number of carbides (TiC, ZrC, and NbC), nitrides (AlN, TiN, and VN), and oxides (CaO, Al_2O_3, and Ce_2O_3) have been tested through externally adding the particles into the melts [16,19,20]. Unfortunately, no breakthroughs have been reported.

An alternative approach to grain refinement of steels is to add rare earths (REs) into the steel melt during ingot casting and continuous casting [21]. This includes cast steels [22], carbon steels [23–27], non-oriented electrical steels [28], Fe-6.5 wt% Si alloy [29], and other engineering steels [30,31]. Although additions of REs in these steels led to significant grain refinement, the actual mechanisms of how rare earths refine the grains and their effects on mechanical properties are still unclear. Commonly, it is considered that RE additions lead to either purification of liquid steels [32], modification of inclusions [32–34], a microalloying effect [35–42], grain refinement [32,34], or their combinations. Previously reported results about the grain refinement during solidification of steels by adding lanthanum or/and cerium are rather inconsistent. There are no commonly accepted theories/models that can be used to fully explain and understand the roles of the REs. The present work reviews the most recently published results on RE-containing steels, aiming to identify the causes of the inconsistency and to understand the roles and mechanisms of lanthanum or/and cerium on the grain refinement during solidification of steels.

Unlike Al- and Mg-based alloys, the solidification process of steels may include direct formation of δ-ferrite (BCC crystal structure) from the liquid, peritectic reaction (δ + liquid→γ), and direct formation of γ-austenite (FCC crystal structure) from the liquid. According to the Fe-Fe_3C binary diagram, when the carbon content is below 0.09 wt%, primary BCC δ-ferrite directly forms from the liquid, followed by a phase transformation from δ-ferrite to FCC γ-austenite. When carbon content is between 0.09 wt% and 0.17 wt%, primary δ-ferrite directly forms from the liquid followed by a peritectic reaction (δ + liquid→γ), and then δ-ferrite transforms to γ-austenite. In these two cases, the nucleation and growth of δ-ferrite define the size of austenite. Hence, the δ-ferrite should be refined during solidification. For steels with carbon content between 0.17 wt% and 0.53 wt%, primary δ-ferrite first forms from the liquid followed by a peritectic reaction. However, after the completion of the peritectic reaction, γ-austenite also directly forms from the liquid. For these steels, the nucleation and growth of both δ-ferrite and γ-austenite determine the size of austenite. Hence, both δ-ferrite and

γ-austenite need to be refined. When the carbon content is over 0.53 wt%, the γ-austenite directly forms from the liquid. Hence, the solidification grain refinement should focus on refining the γ-austenite.

In practice, the non-equilibrium cooling and solute additions significantly influence the critical carbon content as stated above. However, which primary phase—δ-ferrite or γ-austenite—directly forms from the liquid still depends on the contents of carbon and other solutes. The development of effective techniques for grain refinement of steels should use δ-ferrite and γ-austenite as two different targets.

2. Effects of RE Addition on Macrostructure and Microstructure of As-Cast Steels

RE additions, particularly lanthanum (La) or/and cerium (Ce), directly lead to changes of macrostructure and microstructure of as-cast steels, which in turn influences the subsequent forming processes and properties of steel products. Noticeable grain refinement due to the addition of Ce/La in various steels has been reported. The grain refinement efficiency was expressed in terms of either a decrease in the proportion of columnar grains or a reduction in the average grain size, or both. However, there is still a lack of comprehensive investigations of the grain refinement mechanism due to the addition of REs. Major publications on this topic are reviewed as follows.

2.1. RE Additions in Austenitic Steels

For most austenitic steels, γ-austenite directly forms from the liquid during the solidification process. Such austenite can generally be retained at room temperature due to the high content of γ-stabilizers, such as C, Mn, Ni, etc., and relatively fast cooling. Hence, the microstructure of the steels at room temperature can reflect the grain refining efficiency well. Bartlett and co-workers [31] added a Ce-based inoculant, which contained ≈10.0–14.0%Ce, ≈22.0–26.0%Sc, ≈8.0–12.0%Cr, ≈22.0–27.0% Mn, and 1.0%C (weight percent), into an Fe-Mn-Al-C austenitic cast steel. It was found that a 0.1 wt% Ce addition significantly reduced the primary austenite grain size from ≈10–12 mm to 100 μm. Figure 1 shows the macrostructure of the castings. The grain refinement was attributed to the promoted heterogeneous nucleation of austenite on cerium oxide inclusions formed in the melt. Similarly, Haakosen et al [43] reported a reduction in both fraction of columnar structure and in grain size in a cast austenitic manganese steel with 1.42%C, 19.5%Mn, 2.4%Cr, 0.7%Si, 0.03%Al, and 0.15%Ti (weight percent) after the addition of cerium. Figure 2 shows the variation of austenite grain size with the cerium addition level. A critical addition level of ≈0.04–0.05 wt%, over which the grain size was dramatically reduced, was identified. Accordingly, over this critical addition level, the fraction of columnar grains was also significantly decreased, as shown in Figure 3. The authors considered that the grain refinement resulted from the accelerated heterogeneous nucleation of primary austenite via CeO_2, $CeAlO_3$, and Ce_2O_2S particles formed in the liquid steel. However, in both Bartlett's work and Haakosen's work, there was no direct experimental evidence to prove the hypothesis of heterogeneous nucleation on Ce-containing inclusions. Other mechanisms, such as the solute effect, may possibly contribute to the grain refinement. Hence, it is necessary to conduct more comprehensive studies to clarify the roles and mechanisms of REs in austenitic steels.

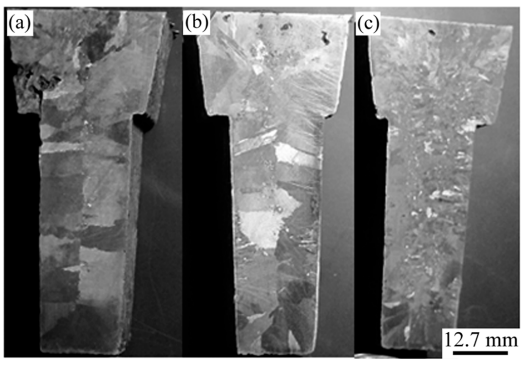

Figure 1. Macrostructure of an as-cast Fe-Mn-Al-C austenitic steel containing different cerium contents: (**a**) 0%, (**b**) 0.05%, and (**c**) 0.1%, reproduced from Reference [31], with permission of Springer, 2016.

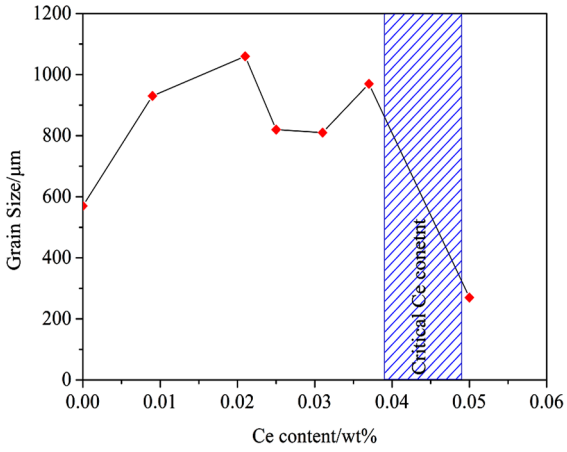

Figure 2. Relationship between the grain size and cerium content in a cast high manganese austenitic steel, reproduced from Reference [43], with permission of AIS Tech, 2011.

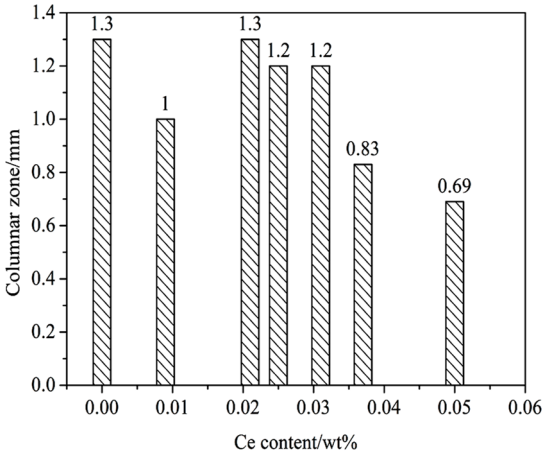

Figure 3. Range of columnar zone versus cerium content in a cast high-manganese austenitic steel, reproduced from Reference [43], with permission of AIS Tech, 2011.

2.2. RE Additions in Ferritic Steels

According to either the lattice disregistry model [15] or the edge-to-edge matching model [44,45], grain refinement efficiency via heterogeneous nucleation is dependent on the crystal structure of the nucleation sites and the metals to be formed. Due to the different crystal structure of austenite and ferrite, the roles of REs may vary with steels. Zhang and co-workers [46] reported that the addition of Ce into a 00Cr17 high-purity ferrite stainless steel resulted in the refinement of the as-cast macrostructure [46]. As shown in Figure 4, although the columnar structure was refined with an increase in Ce addition, no equiaxed grains formed in this steel. Such result indicated that, at least, heterogeneous nucleation did not occur within the melt. However, Xu and co-workers [47] reported an increase in the equiaxed grain zone from 3% to 33% in an as-cast 430 ferritic stainless steel after adding 0.073 wt% Ce as shown in Figure 5 [47]. However, the refinement efficiency was very marginal. Xu and co-workers [47] considered that both the heterogeneous nucleation of ferrite on RE sulfide/oxide particles and the solute effect of Ce contributed to the reduction in columnar fraction in the ingots. Similar to the works on austenitic steels, no direct experimental evidence has been reported to verify these hypotheses.

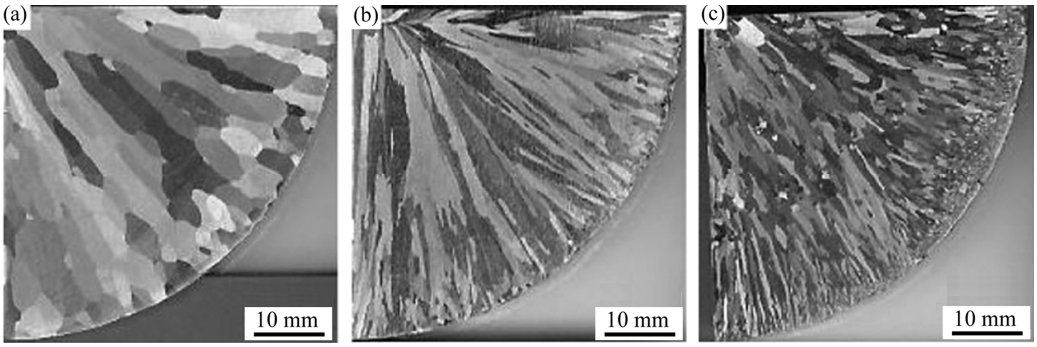

Figure 4. As-cast macrostructure of a 00Cr17 high-purity ferrite stainless steel with different cerium additions: (**a**) 0%, (**b**) 0.02%, and (**c**) 0.08%, reproduced from Reference [46], with permission of Cailiao Rechuli Xuebao/Transactions of Materials and Heat Treatment, 2011.

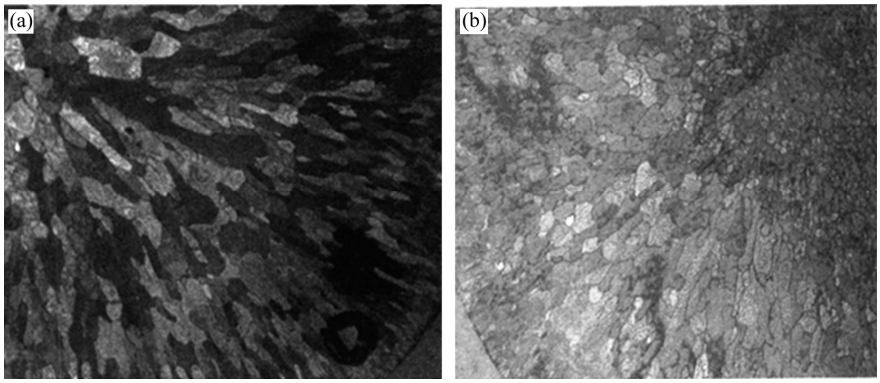

Figure 5. As-cast microstructure of an as-cast 430 ferrite stainless steel: (**a**) without RE, and (**b**) with 0.073% RE [47], with permission of Journal of the Chinese Society of Rare Earths/Journal of the Chinese Rare Earth Society, 2006.

2.3. RE Additions in Plain Carbon Steels

The most common use of REs was in commercial steels, including plain carbon steels. Because of the different carbon contents, the grain refining efficiency due to the RE additions also varied. Tuttle [25,48–50] investigated the effects of RE additions on the microstructure and properties of 1010 and 1030 steel (plain carbon steels) and found that the appropriate additions of La and Ce refined the as-cast microstructure. In order to clarify the grain-refining mechanism, cast samples with various RE addition levels were characterized in terms of grain size, microstructural morphology, and crystallographic features using a scanning electron microscope (SEM) and transmission electron microscope (TEM) with an energy dispersive spectrometer (EDS). It was concluded that simple RE oxides or sulfides were unable to promote the heterogeneous nucleation of δ-ferrite, but more complex RE oxides and/or oxysulfides possibly acted as the nucleants. Unfortunately, such oxides/oxysulfides were not identified in Tuttle's work.

Grain refinement via La addition was also observed by Wang et al. [51] in an ASTM A216 steel (a plain carbon steel). The team calculated the lattice mismatch using the two-dimensional disregistry theory and indicated that the La inclusions of La_2O_3, La_2O_2S, and LaS could act as the heterogeneous nucleation sites of δ-ferrite. However, these inclusions were not experimentally observed. Similar work was done by Li et al. [52] who added 0.16 wt% cerium into a 1045 carbon steel by in-mold addition and observed a remarkable increase in the equiaxed grain zone from 16 ± 2% to 64 ± 2% and a reduction in the average grain size from 762 μm to 541 μm. Then, the effects of cerium addition on the degree of undercooling in a pure iron and the 1045 steel were investigated using the levitation melting method while the surface tension of the levitated droplets was measured. However, based on the results, it was

indicated that cerium solute redistribution during the solidification is the dominant factor contributing to the refinement of the as-cast structure of the 1045 steel.

2.4. RE Additions in other Engineering Steels

REs have also been widely used in engineering alloy steels. Wang et al. [53] observed a reduction in proportion of the columnar zone from 90.7% to 58.1% in an advanced low alloy steel (no composition of the steel is indicated in the reference) after adding 0.12 wt% mixture of La and Ce. Guo and Suito [23,24] investigated the influence of dissolved Ce and the primary particles of Ce_2O_3 and CeS on the as-cast macrostructure and microstructure of a 0.20%C–0.02%P steel. They found that the primary and secondary dendrite arm spacing decreased with an increase in either the cerium content or the amount of Ce_2O_3 and CeS particles. However, the fraction of equiaxed grains was independent of the soluble cerium content even though it was increased owing to the addition of Ce_2O_3 or CeS particles.

Gao's work [30] also indicated that adding 0.015 wt% mixed RE (mainly containing 30% La and 65% Ce) led to a noticeable grain refinement of an as-cast H13 steel as shown in Figure 6. However, further addition of RE had little effect on the grain size. Detailed characterization of the as-cast H13 steel using both EDS analysis and TEM electron diffraction identified a Ce oxysulfide, Ce_2O_2S, in the steel. The authors further calculated the lattice mismatch between the Ce_2O_2S and the ferritic matrix according to the two-dimensional lattice disregistry theory, identifying a low mismatch of 3.5%. Hence it was concluded that the grain refinement was attributed to the heterogeneous nucleation of ferrite on the Ce_2O_2S inclusion. However, H13 steel contains 0.32 to 0.45 wt% carbon. During solidification process, it is questionable how much δ-ferrite can directly form from the liquid. In addition, explanation of the constant grain size when a higher amount of RE was added is also a challenge.

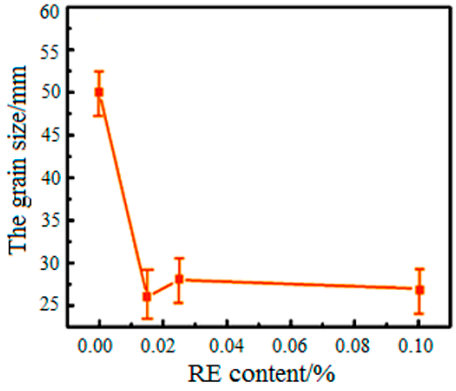

Figure 6. Variation of average grain sizes of as-cast H13 steel with additions of RE, reproduced from Reference [30], with permission of Springer, 2015.

2.5. Discussion

To understand the actual roles of REs in grain refinement in different steels, the above-mentioned results are summarized in Table 1. These results lead to the following conclusions:

- The addition of REs led to a reduction in either fraction of columnar grains or the grain size of equiaxed grains or both in the as-cast steels.
- The grain-refining mechanism of RE additions seemed similar in ferritic steels, austenitic steels, and engineering steels even though the grain refining efficiency varies in different steels.
- In terms of grain refinement, the roles of lanthanum and cerium seemed similar in the as-cast steels.
- The most generally accepted explanation of the grain refinement was heterogeneous nucleation of either δ-ferrite or γ-austenite on the RE inclusions, including oxides, sulfides and oxysulfides, and solute effects.

These conclusions are also associated with a few questions:

- What are the predominant factors that led to the reduction in the fraction of columnar grains, and what are the factors that are responsible for the equiaxed grain refinement? To answer these questions, the roles of the inoculant and solutes in the solidification of δ-ferrite and γ-austenite need to be comprehensively investigated though crystallographic and thermodynamic calculation followed by experimental verification.
- What are the actual causes of significant difference in the grain-refining efficiency in different steels? For example, Ce addition led to a grain size reduction from 10–12 mm down to 100 μm in the Fe-Mn-Al-C cast steel [31]; however, the grain refining efficiency in another austenitic manganese steel [43] is much smaller. In the 00Cr17 stainless steel [46], Ce addition only led to refinement of the columnar grains, but the grain size was slightly reduced in the 430 ferritic stainless steel [47]. Grain refining efficiency depends on various factors, such as the casting condition and cooling rate. To clarify these inconsistent results, the effects of Ce (or other solutes) additions need to be investigated in different steels under the same casting conditions and cooling rate. In addition, the growth restriction factor of Ce (or other solutes) should be more carefully calculated in various steel systems.
- Addition of REs in steels resulted in the formation of various inclusions as mentioned above. The question is: which inclusions are more effective in promoting the heterogeneous nucleation of the BCC δ-ferrite and for the FCC γ-austenite? What are the key factors that govern the formation of different types of RE-containing inclusions? How do the oxygen content, sulfur content, and their relative amount (the ratio of oxygen content to sulfur content) affect the formation of the inclusions? To answer these questions, considerable research work needs to be conducted. For example, special alloys should be designed so that the δ-ferrite formed directly from the liquid at high temperature can be retained at room temperature without subsequent phase transformations. The similar alloys are required to keep the γ-austenite directly formed from the liquid to room temperature. In addition, types of RE inclusions formed in these specially designed alloys containing various level of oxygen and sulfur should be comprehensively investigated through thermodynamic calculation and experimental observation. The graining refining efficiencies of different RE inclusions in both δ-ferrite and γ-austenite can be crystallographically predicted and experimentally confirmed under the same casting conditions.
- How does the chemical composition of steels influence the grain-refining efficiency of the RE additions? To answer this question, the grain refinement through RE additions needs to be studied in wide range of steels under the same casting conditions, together with a study to understand the affinity of RE to the alloying elements in the steels in addition to oxygen and sulfur.

In addition to these questions, there is also lack of direct experimental evidence to verify the hypothesis that the RE oxides/sulfides/oxysulfides are effective heterogeneous nucleation sites for either δ-ferrite or γ-austenite. In terms of the solute effect of the REs, the actual growth restriction factors (Q-values) of the REs in both ferrite and austenite are also not available. Hence, due to the importance of REs in steels, it is necessary to conduct comprehensive studies to understand the roles and mechanisms of REs in steels, particularly in grain refinement.

Table 1. Published works on grain refinement of as-cast steels through addition of lanthanum or/and cerium.

REs	Steels	Mold Type	Grain Refining Efficiency	Mechanism	Research Type	References	Shortcomings
Ce	00Cr17 high-purity ferrite stainless steel	No information is given	The columnar structure was refined.	-	Experimental	[46]	No explanation was provided.
La and Ce	An advanced low alloy steel (No composition is indicated)	No information is given	The columnar grains zone reduced from 90.7% to 58.1%.	-	Experimental	[53]	
Ce	Fe-Mn-Al-C cast steel	Air-set silica sand mold coated with zircon	The primary austenite grain size was significantly refined from 10~12 mm to 100 μm.	Heterogeneous nucleation of γ-austenite on cerium oxide inclusions.	Experimental	[31]	Direct experimental evidence is needed to verify these hypotheses.
Ce	Cast austenitic manganese steel	Olivine sand mold	The fraction of columnar structure decreased and the grains were refined.	Heterogeneous nucleation of primary austenite on either CeO_2 or $CeAlO_3$ or Ce_2O_2S inclusions.	Experimental	[43]	
Ce	430 ferrite stainless steel	No information is given	The equiaxed grain zone was enlarged from 3% to 33% and both the columnar and the equiaxed grains were refined.	Both the heterogeneous nucleation on RE sulfide and oxide and the solute effect of cerium contributed to the grain refinement.	Experimental	[47]	
La	ASTM A216 steel (plain carbon steel)	No information is given	La refined the grains significantly.	La_2O_3, La_2O_2S and LaS acted as the heterogeneous nucleation sites for δ-ferrite and the dissolved lanthanum in the molten steel increased the degree of supercooling.	Experimental	[51]	
Ce	1045 carbon steel	Zircon sand mold	Cerium enlarged the equiaxed grain zone and reduced the primary and secondary dendrite arm spacing in the cast alloys.	Cerium solute redistribution during the solidification was the dominant factor in the refinement of the as-cast structure.	Experimental	[52]	
Ce	0.20%C–0.02%P steel	Not molded, melted in Al_2O_3 crucible then quenched in water	The primary and secondary dendrite arm spacings were decreased and the equiaxed grain zone was enlarged.	The solute effect of Ce and the heterogeneous nucleation of ferrite on Ce_2O_3 and CeS particles were responsible for the grain refinement.	Experimental	[23,24]	
La and Ce	1010 and 1030 steel (plain carbon steels)	Silica based molding sand mold	The RE additions refined the as-cast microstructure.	The complex RE oxides or oxysulfides acted as the heterogeneous nucleation sites for δ-ferrite.	Experimental	[25,48–50]	
30% La and 65% Ce	H13 steel	No information is given	The average grain size was reduced from 50 μm to 25 μm.	Ce_2O_2S could act as the heterogeneous nucleation sites for δ-ferrite.	Experimental	[30]	Direct experimental evidence is needed to verify the assumption. In addition, it is also questionable whether δ-ferrite directly formed from the liquid.

3. Grain Refinement Mechanisms of Rare Earths in Steels

3.1. State of Rare Earths in Steels

Because of the high affinity with oxygen and sulfur, the externally added rare earth elements tend to chemically react with oxygen first and then with sulfur to form various RE inclusions in steel melts depending on the concentrations of oxygen and sulfur. If the content of REs and other elements is sufficient, REs can also react with P or other impurities to form different compounds. If the oxygen and sulfur contents are low, and/or the amount of REs added is higher, the remaining REs would possibly dissolve in the ferrite/austenite forming solid solution. In most industrial steels, the externally added RE elements highly likely form oxides, oxysulfides, or sulfides, and also possibly exist as solutes in the solid solution [54–56]. Hence, it is generally considered that grain refinement of steels by RE additions is attributed to either the heterogeneous nucleation on RE inclusions [25,30,31,43,48–52], a solute effect [52], or both [47,51].

3.2. Heterogeneous Nucleation of Ferrite and/or Austenite on RE Inclusions

3.2.1. Formation of Rare Earth Inclusions in Molten Steel

Adding lanthanum and cerium into molten steel leads to the formation of various compounds. Figure 7 shows the equilibrium lines showing the affinity of a few alloying elements to oxygen and sulfur in liquid iron at 1600 °C [33]. It can be seen that except for Ca, La and Ce have the highest tendency to form oxides and sulfides. Generally, oxides form prior to sulfides. Considerable studies [57–59] verified the formation sequence as: RE oxides > RE oxysulfides > RE sulfides. The typical oxide is RE_2O_3. The oxysulfide is an intermediate product during the transition from deoxygenation to desulfuration by cerium and lanthanum. The variety and distribution of the RE oxysulfides rely on the contents of oxygen and sulfur and the condensate depression of the molten steel. The RE_2O_2S commonly forms. The type of RE sulfides is related to the ratio of RE content to S content, i.e., the value of [RE]/[S], in the molten steel. Typical sulfides are RE_2S_3, RE_3S_4, and RES. Figure 8 is the inclusion precipitation diagram for the Fe-Ce-O-S system at 1627 °C, showing the equilibrium reaction of Ce with oxygen and sulfur and the formation sequence of Ce-containing inclusions [33]. The melting temperatures of all these RE inclusions are generally above the solidification temperature of steel melts. Thus, they have the potential to act as the heterogeneous nucleation sites for the primary phases of steels, leading to grain refinement.

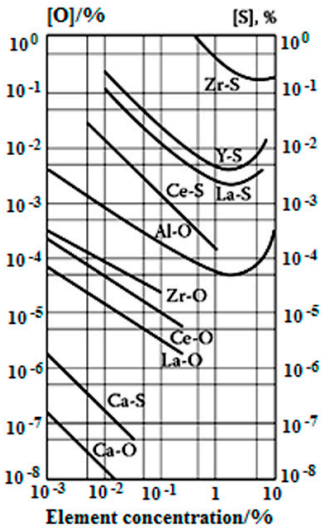

Figure 7. Equilibrium curves showing the affinity of a few alloying elements to oxygen and sulfur in iron at 1600 °C, reproduced from Reference [33], with permission of Springer, 2016.

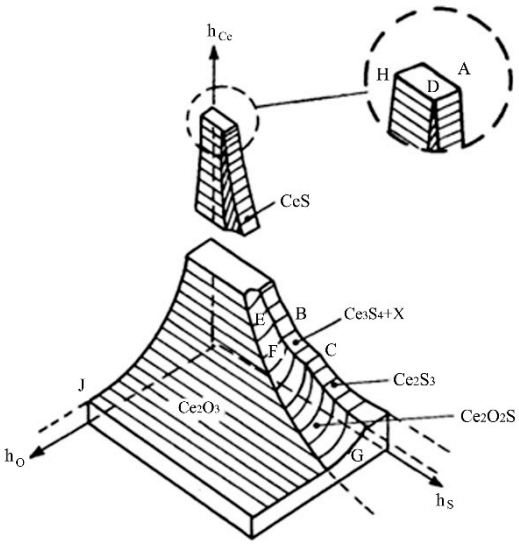

Figure 8. Inclusion precipitation diagram for the Fe-Ce-O-S system at 1627 °C. h_{Ce}, h_O, and h_S represent Henrian activities of cerium, oxygen, and sulfur, respectively, reproduced from Reference [33], with permission of Springer, 2016.

3.2.2. Models/Theories for Evaluation of Heterogeneous Nucleation Potency

In order to facilitate the heterogeneous nucleation, a valid nucleating agent (also termed a nucleant or inoculant) should fulfill the following three essential conditions [48,60]: (1) they are solid at the solidification temperature of the metal melt, (2) they are thermodynamically stable in the melt, and (3) they are wetted by the melt (low wetting angle between the melt and the solid). In addition, according to the classic heterogeneous nucleation theory, to improve the nucleation rate and therefore increase the grain refinement efficiency, the interfacial energy between the nucleating agents and the nucleus formed on the agents is required to be as low as possible. Generally, there are a number of factors influencing the interfacial energy [16], such as crystallographic atomic matching and the difference in electronegativity between the nucleating agents and the nucleation phase. Because it is rather difficult to accurately calculate the interfacial energy, crystallographic atomic matching is usually used to evaluate the nucleation potency of particles. This is based on two assumptions. One is that the coherent or semi-coherent interface between two crystalline solids corresponds to lower interfacial energy than the incoherent interface, and another is that the minimization of the interfacial energy of coherent or semi-coherent interface can be achieved through maximization of atomic matching across the interface. In the past few decades, several models have been developed to examine the nucleation potency and some have been successful in evaluating the grain refinement efficiency. This includes the lattice disregistry approach [16,61], the electrostatic action theory [62,63], and the edge-to-edge matching (E2EM) model [64–66].

Lattice Disregistry Approach

The lattice disregistry approach is the earliest approach to evaluate the grain refinement potency from crystallographic point view simply based on the lattice parameters of the nucleation agent and phase to be formed on it. In 1952, Turnbull and Vonnegut [61] proposed that the grain refinement potency of a nucleating agent depended on the lattice disregistry between the nucleating agent and the nucleation phase. The one-dimensional disregistry was defined as follows:

$$\delta = \frac{|a_s - a_n|}{a_n} \quad (1)$$

where δ is the lattice disregistry and the parameters of a_n and a_s denote the lattice constant in the low index crystal planes of the nucleus and the nucleating agent, respectively. A smaller value of δ implies a lower interfacial energy, which indicates the higher grain refinement efficiency. Because this model is limited to the case that the nucleus and the nucleation particles have the same atomic configuration on the specific low index plane, it has been rarely used.

In 1970, Bramfitt [16] proposed the two-dimensional disregistry model on the basis of the one-dimensional disregistry. The lattice disregistry is expressed as follows [16]:

$$\delta_{(hkl)_n}^{(hkl)_s} = \sum_{i=1}^{3} \frac{\left| d_{[uvw]_s^i} \cos\theta - d_{[uvw]_n^i} \right|}{d_{[uvw]_n^i}} \times 100\% \quad (2)$$

where δ is the lattice disregistry, $(hkl)_s$ is a low-index plane of the nucleating agent, $[uvw]_s$ is a low-index direction in the $(hkl)_s$, $(hkl)_n$ is a low-index plane of the nucleus, $[uvw]_n$ is a low-index direction in $(hkl)_n$, $d_{[uvw]_n}$ is the interatomic spacing along $[uvw]_n$, $d_{[uvw]_s}$ is the interatomic spacing along $[uvw]_s$, and θ is the angle between $[uvw]_s$ and $[uvw]_n$.

Bramfitt [16] also proposed a criterion for evaluating the grain refinement potency: the most effective grain refinement can be achieved when the δ-value is below 6%; the agents are moderately effective when the δ-value is in between 6% and 12%; and if the δ-value is over 12%, the agent almost cannot refine the grains.

In the past few decades, this model has been widely used. The grain refinement potency of the RE oxides, oxysulfides, and sulfides for δ-ferrite and/or γ-austenite primary phase during solidification of steels have been examined using the two-dimensional disregistry model [25,30,48,51,67–69]. Pan et al. [70] calculated the two-dimensional disregistry between the potential nucleants, Ce_2O_3 and La_2O_3, and the primary phases (δ-ferrite and γ-austenite) at 1500 °C. The calculated δ values were: $\delta_{\text{ferrite}-Ce_2O_3} = 4.49\%$, $\delta_{\text{ferrite}-La_2O_3} = 3.34\%$, $\delta_{\text{austenite}-Ce_2O_3} = 14.21\%$, and $\delta_{\text{austenite}-La_2O_3} = 13.17\%$. In terms of the Bramfitt's criteria [16], Ce_2O_3 and La_2O_3 could effectively promote heterogeneous nucleation of δ-ferrite, but not for γ-austenite. However, the disregistry between the La_2O_3 and δ-ferrite calculated by Tuttle [25,48] was around 30%, which is much higher than that of the generally accepted level for effective nucleation. Tables 2 and 3 list the published δ-values between various RE inclusions and primary δ-ferrite/γ-austenite. From these data, the following approximate predictions can be made:

- Ce_2O_3 is a moderately effective grain refiner for δ-ferrite.
- The heterogeneous nucleation potency of Ce_2O_2S for δ-ferrite is inconsistent. According to reference [68], the efficiency of Ce_2O_2S is moderate. However, in the work of Reference [23], it is prominent.
- All La_2O_3, La_2O_2S and LaS are effective grain refiners for δ-ferrite and the refining potency is in the order of LaS > La_2O_2S > La_2O_3.
- Both Ce_2O_3 and Ce_2O_2S can refine γ-austenite and the potency of Ce_2O_3 is slightly better than that of Ce_2O_2S.
- The heterogeneous nucleation potency of Ce_2O_3 for γ-austenite is inconsistent based on different published works, so is Ce_2O_2S.
- CeS cannot refine γ-austenite.
- Both La_2O_3 and La_2O_2S can act as the heterogeneous nucleation sites of the primary γ-austenite. The efficiency of La_2O_2S is prominent, but the La_2O_3 is moderate.

Table 2. Planar misfits between Ce_2O_3, Ce_2O_2S, La_2O_3, La_2O_2S, LaS, and δ-Fe.

$(0001)_{Ce_2O_3}(100)_{\delta-Fe}$				$(0001)_{Ce_2O_3}(110)_{\delta-Fe}$				$(0001)_{Ce_2O_3}(111)_{\delta-Fe}$				**Reference**
$[uvtw]_{Ce_2O_3}$	$[\bar{1}2\bar{1}0]$	$[10\bar{1}0]$	$[\bar{2}110]$	$[uvtw]_{Ce_2O_3}$	$[\bar{1}2\bar{1}0]$	$[10\bar{1}0]$	$[\bar{2}110]$	$[uvtw]_{Ce_2O_3}$	$[\bar{1}2\bar{1}0]$	$[10\bar{1}0]$	$[\bar{2}110]$	[68]
$[uvw]_{\delta-Fe}$	[011]	[021]	$[01\bar{1}]$	$[uvw]_{\delta-Fe}$	$[\bar{1}10]$	$[\bar{1}12]$	$[\bar{2}21]$	$[uvw]_{\delta-Fe}$	$[\bar{1}01]$	$[\bar{1}10]$	$[\bar{2}11]$	
δ		8.1%		δ		18.3%		δ		37.6%		
$(0001)_{Ce_2O_2S}(100)_{\delta-Fe}$				$(0001)_{Ce_2O_2S}(110)_{\delta-Fe}$				$(0001)_{Ce_2O_2S}(111)_{\delta-Fe}$				Reference
$[uvtw]_{Ce_2O_2S}$	$[\bar{1}2\bar{1}0]$	$[10\bar{1}0]$	$[\bar{2}110]$	$[uvtw]_{Ce_2O_2S}$	$[\bar{1}2\bar{1}0]$	$[10\bar{1}0]$	$[\bar{2}110]$	$[uvtw]_{Ce_2O_2S}$	$[\bar{1}2\bar{1}0]$	$[10\bar{1}0]$	$[\bar{2}110]$	[68]
$[uvw]_{\delta-Fe}$	[011]	[021]	$[01\bar{1}]$	$[uvw]_{\delta-Fe}$	$[\bar{1}10]$	$[\bar{1}12]$	$[\bar{2}21]$	$[uvw]_{\delta-Fe}$	$[\bar{1}01]$	$[\bar{1}10]$	$[\bar{2}11]$	
δ		10.3%		δ		17.0%		δ		38.8%		
$(0001)_{Ce_2O_2S}(100)_{\delta-Fe}$				$(0001)_{Ce_2O_2S}(110)_{\delta-Fe}$				$(0001)_{Ce_2O_2S}(111)_{\delta-Fe}$				Reference
$[uvtw]_{Ce_2O_2S}$	[1210]	[2110]	[1010]	$[uvtw]_{Ce_2O_2S}$	[1210]	[2110]	[1010]	$[uvtw]_{Ce_2O_2S}$	[1210]	[1100]	[2110]	[30]
$[uvw]_{\delta-Fe}$	[010]	[011]	[001]	$[uvw]_{\delta-Fe}$	[001]	[111]	[110]	$[uvw]_{\delta-Fe}$	[110]	[121]	[011]	
δ		55.3%		δ		53.5%		δ		3.5%		
$(0001)_{La_2O_3}(111)_{\delta-Fe}$				$(0001)_{La_2O_2S}(111)_{\delta-Fe}$				$(111)_{LaS}(111)_{\delta-Fe}$				Reference
$[uvtw]_{La_2O_3}$	[2110]	$[\bar{1}100]$	$[\bar{1}2\bar{1}0]$	$[uvtw]_{La_2O_2S}$	$[\bar{2}110]$	$[\bar{1}100]$	$[\bar{1}2\bar{1}0]$	$[uvw]_{LaS}$	$[\bar{1}01]$	$[\bar{2}11]$	$[\bar{1}10]$	[51]
$[uvw]_{\delta-Fe}$	$[\bar{1}01]$	$[\bar{2}11]$	$[\bar{1}10]$	$[uvw]_{\delta-Fe}$	$[\bar{1}01]$	$[\bar{2}11]$	$[\bar{1}10]$	$[uvw]_{\delta-Fe}$	$[\bar{1}01]$	$[\bar{2}11]$	$[\bar{1}10]$	
δ		3.34%		δ		2.6%		δ		0.6%		

Table 3. Planar misfits between Ce_2O_3, Ce_2O_2S, La_2O_3, La_2O_2S, CeS, and γ-Fe.

$(0001)_{Ce_2O_3}(100)_{\gamma-Fe}$				$(0001)_{Ce_2O_3}(110)_{\gamma-Fe}$				$(0001)_{Ce_2O_3}(111)_{\gamma-Fe}$				**Reference**
$[uvtw]_{Ce_2O_3}$	$[\bar{1}2\bar{1}0]$	$[10\bar{1}0]$	$[\bar{2}110]$	$[uvtw]_{Ce_2O_3}$	$[\bar{1}2\bar{1}0]$	$[10\bar{1}0]$	$[\bar{2}110]$	$[uvtw]_{Ce_2O_3}$	$[\bar{1}2\bar{1}0]$	$[10\bar{1}0]$	$[\bar{2}110]$	
$[uvw]_{\gamma-Fe}$	[010]	[031]	[001]	$[uvw]_{\gamma-Fe}$	$[00\bar{1}]$	$[\bar{1}1\bar{1}]$	$[\bar{1}10]$	$[uvw]_{\gamma-Fe}$	$[\bar{1}01]$	$[\bar{2}11]$	$[\bar{1}10]$	[69]
δ		7.7%		δ		13.3%		δ		21.3%		
$(0001)_{Ce_2O_3}(100)_{\gamma-Fe}$				$(0001)_{Ce_2O_3}(110)_{\gamma-Fe}$				$(0001)_{Ce_2O_3}(111)_{\gamma-Fe}$				Reference
$[uvtw]_{Ce_2O_3}$	$[\bar{1}2\bar{1}0]$	$[\bar{1}100]$	$[\bar{2}110]$	$[uvtw]_{Ce_2O_3}$	$[\bar{1}2\bar{1}0]$	$[\bar{1}100]$	$[\bar{2}110]$	$[uvtw]_{Ce_2O_3}$	$[\bar{1}2\bar{1}0]$	$[\bar{1}100]$	$[\bar{2}110]$	
$[uvw]_{\gamma-Fe}$	[010]	[031]	[011]	$[uvw]_{\gamma-Fe}$	[100]	$[\bar{1}12]$	$[\bar{1}10]$	$[uvw]_{\gamma-Fe}$	$[\bar{1}01]$	$[\bar{2}11]$	$[\bar{1}10]$	[71]
δ		15.8%		δ		13.0%		δ		5.4%		

Table 3. *Cont.*

$(0001)_{Ce_2O_2S}(100)_{\gamma-Fe}$				$(0001)_{Ce_2O_2S}(110)_{\gamma-Fe}$				$(0001)_{Ce_2O_2S}(111)_{\gamma-Fe}$				Reference
$[uvtw]_{Ce_2O_2S}$	$[\bar{1}2\bar{1}0]$	$[10\bar{1}0]$	$[\bar{2}110]$	$[uvtw]_{Ce_2O_2S}$	$[\bar{1}2\bar{1}0]$	$[10\bar{1}0]$	$[\bar{2}110]$	$[uvtw]_{Ce_2O_2S}$	$[\bar{1}2\bar{1}0]$	$[10\bar{1}0]$	$[\bar{2}110]$	
$[uvw]_{\gamma-Fe}$	[010]	[031]	[001]	$[uvw]_{\gamma-Fe}$	$[00\bar{1}]$	$[\bar{1}1\bar{1}]$	$[\bar{1}10]$	$[uvw]_{\gamma-Fe}$	$[\bar{1}0\bar{1}]$	$[\bar{2}11]$	$[\bar{1}10]$	[69]
δ		10.2%		δ		13.5%		δ		31.1%		
$(0001)_{Ce_2O_2S}(100)_{\gamma-Fe}$				$(0001)_{Ce_2O_2S}(110)_{\gamma-Fe}$				$(0001)_{Ce_2O_2S}(111)_{\gamma-Fe}$				Reference
$[uvtw]_{Ce_2O_2S}$	$[\bar{1}2\bar{1}0]$	$[\bar{1}100]$	$[\bar{2}110]$	$[uvtw]_{Ce_2O_2S}$	$[\bar{1}2\bar{1}0]$	$[\bar{1}100]$	$[\bar{2}110]$	$[uvtw]_{Ce_2O_2S}$	$[\bar{1}2\bar{1}0]$	$[\bar{1}100]$	$[\bar{2}110]$	
$[uvw]_{\gamma-Fe}$	[010]	[031]	[011]	$[uvw]_{\gamma-Fe}$	[100]	$[\bar{1}12]$	$[\bar{1}10]$	$[uvw]_{\gamma-Fe}$	$[\bar{1}01]$	$[\bar{2}11]$	$[\bar{1}10]$	[71]
δ		14.9%		δ		14%		δ		10.3%		
$(0001)_{La_2O_3}(100)_{\gamma-Fe}$				$(0001)_{La_2O_3}(110)_{\gamma-Fe}$				$(0001)_{La_2O_3}(111)_{\gamma-Fe}$				Reference
$[uvtw]_{La_2O_3}$	$[\bar{1}2\bar{1}0]$	$[\bar{1}100]$	$[\bar{2}110]$	$[uvtw]_{La_2O_3}$	$[\bar{1}100]$	$[\bar{2}110]$	$[\bar{2}110]$	$[uvtw]_{La_2O_3}$	$[\bar{1}2\bar{1}0]$	$[\bar{1}100]$	$[\bar{2}110]$	
$[uvw]_{\gamma-Fe}$	[010]	[031]	[011]	$[uvw]_{\gamma-Fe}$	[100]	$[\bar{1}12]$	$[\bar{1}10]$	$[uvw]_{\gamma-Fe}$	$[\bar{1}01]$	$[\bar{2}11]$	$[\bar{1}10]$	[72]
δ		15.49%		δ		12.51%		δ		6.7%		
$(0001)_{La_2O_2S}(100)_{\gamma-Fe}$				$(0001)_{La_2O_2S}(110)_{\gamma-Fe}$				$(0001)_{La_2O_2S}(111)_{\gamma-Fe}$				Reference
$[uvtw]_{La_2O_2S}$	$[\bar{1}2\bar{1}0]$	$[\bar{2}110]$	$[\bar{1}010]$	$[uvtw]_{La_2O_2S}$	$[\bar{1}2\bar{1}0]$	$[\bar{2}110]$	$[\bar{1}010]$	$[uvtw]_{La_2O_2S}$	$[\bar{1}2\bar{1}0]$	$[\bar{1}100]$	$[\bar{2}110]$	
$[uvw]_{\gamma-Fe}$	[010]	[012]	[001]	$[uvw]_{\gamma-Fe}$	$[00\bar{1}]$	$[\bar{1}1\bar{1}]$	$[\bar{1}10]$	$[uvw]_{\gamma-Fe}$	$[\bar{1}10]$	$[\bar{2}11]$	$[\bar{1}01]$	[73]
δ		5.42%		δ		23.82%		δ		55.69%		
$(100)_{CeS}(100)_{\gamma-Fe}$				$(100)_{CeS}(110)_{\gamma-Fe}$				$(100)_{CeS}(111)_{\gamma-Fe}$				Reference
$[uvw]_{CeS}$	[001]	[011]	[010]	$[uvw]_{CeS}$	[001]	[011]	[010]	$[uvw]_{CeS}$	[001]	[011]	[010]	
$[uvw]_{\gamma-Fe}$	[001]	[011]	[010]	$[uvw]_{\gamma-Fe}$	$[\bar{1}10]$	$[\bar{1}11]$	[100]	$[uvw]_{\gamma-Fe}$	$[\bar{1}2\bar{1}]$	$[\bar{2}11]$	$[\bar{1}10]$	[71]
δ		48.7%		δ		26.5%		δ		30.3%		
$(100)_{CeS}(100)_{\gamma-Fe}$				$(100)_{CeS}(110)_{\gamma-Fe}$				$(100)_{CeS}(111)_{\gamma-Fe}$				Reference
$[uvw]_{CeS}$	[001]	[011]	[010]	$[uvw]_{CeS}$	[001]	[011]	[010]	$[uvw]_{CeS}$	[001]	[011]	[010]	
$[uvw]_{\gamma-Fe}$	[001]	[011]	[010]	$[uvw]_{\gamma-Fe}$	$[\bar{1}10]$	$[\bar{1}11]$	[100]	$[uvw]_{\gamma-Fe}$	$[\bar{1}2\bar{1}]$	$[\bar{2}11]$	$[\bar{1}10]$	[74]
δ		50.7%		δ		27.3%		δ		31.2%		

The data in Tables 2 and 3 also show that the δ-values closely depend on the selection of the low index planes. Because no clear criteria for selecting the low index planes and directions were specified in the two-dimensional disregistry model, the calculated δ-values are highly scattered. Even for a given system of plane and direction, the δ-values were also inconsistent. For example, the smallest δ-value for Ce_2O_2S and δ-ferrite calculated by Hao and co-workers [68] was 10.3%, which corresponds to a moderate grain refining efficiency of Ce_2O_2S for δ-ferrite. However, Gao and team [30] calculated the smallest δ-value was 3.5%, implying a high grain refining efficiency of Ce_2O_2S for δ-ferrite. Hence, although the two-dimensional lattice disregistry model has been widely used, further improvement of the model is needed. In addition, this model is limited to the system of the nucleant and the metal with simple crystal structures. For the nucleants that have a more complicated crystal structure, the calculation of the lattice disregistry would be inaccurate because atoms may not occupy the lattice points in this type of crystal structure. Furthermore, the proposed criterion also sometimes fails. For example, Liang and co-workers' experimental works [75,76] showed different grain refinement efficiency of various nucleants even though they were associated with the same disregistry.

Electrostatic Action Theory

The electrostatic action theory was proposed in 1969 [62,63] based on the calculation of the electronic work functions of the nucleus, liquid phase, and the nucleation agent. Due to the difficulty and even impossibility regarding the accurate calculation of the electronic work function for crystals with complicated structures, the application of this electrostatic action theory has been very limited. To simplify the theory, Liang and co-workers combined Yu's empirical electron theory of solids and molecules (EET theory) and Cheng's improved TFD (Thomas-Fermi-Dirac) model, and proposed a valence electron model [75,76] for heterogeneous nucleation. This model is composed of the hybridization stable layer for nucleation phase cells, the dual crystal lattice electron layer for nucleation phase and the nucleating agent, and the hybridization stable layer for nucleating agent. Moreover, a criterion for evaluation of the grain refinement potency was constructed according to the following equation:

$$\Delta\zeta = \left| \frac{2(\zeta_n - \zeta_s)}{\zeta_n + \zeta_s} \right| \quad (3)$$

where $\Delta\zeta$ is defined as a characteristic parameter, and ζ_n and ζ_s are lattice electron migration potentials of nucleation phase and nucleating agent respectively. Bigger values of $\Delta\zeta$ implies greater atomic migration rate and more stable combination between the nucleation phase and the nucleating agent, which indicates a higher grain refinement potency of the nucleating agent.

Liang et al. analyzed the heterogeneous nucleation potency of VC, NbC, TiC, TaC, ZrC, and CaS particles for the non-equilibrium solidification of an austenite steel [75] and that of ZrC, TiC, TiN, and TiO in the process of Au solidification [76] using the model and criterion. The results agreed well with the experiments. Pan and co-workers [70,77] compared the validity of the two-dimensional disregistry model and the valence electron model in terms of the grain refinement efficiency for the two possible primary phases, δ-ferrite or ã-austenite, in steels, and found very inconsistent results. Hence, further refinement of the valence electron model is necessary.

The Edge-to-Edge Matching (E2EM) Model

The edge-to-edge matching model [64–66] was originally developed by M-X Zhang and P.M. Kelly for understanding and predicting the orientation relationships (ORs) and habit plane between two adjacent phases in diffusion-controlled solid-solid phase transformations. This model has been the unique crystallography model that has been successful in interpreting the mechanism of grain refinement in cast metals and identifying new grain refiners in Al, Mg, and their alloys [78–81].

Like all other crystallographic models [82–86], the E2EM model is also based on the assumption that the crystallographic features of the interface between two phases are defined by the minimization of interfacial energy, which can be achieved through maximization of atomic matching across the

interface. The model emphasizes the actual atomic matching between two phases rather than lattice matching specified in the two-dimensional disregistry model. Figure 9 schematically demonstrates an interface that forms in the manner of the edge-to-edge matching [66]. Generally, the primary requirement of the model is the atomic matching along the parallel atomic rows between two phases. The matching atomic rows should be close-packed (CP) or nearly CP directions with low interatomic spacing misfit (f_r). The matching rows can be either straight or zigzag, but the E2EM model requires that straight rows match with straight rows, while zigzag rows match with zigzag rows, as is seen in Figure 10 [64]. Such rows are termed as the matching directions. In addition, it also requires a pair of CP or nearly CP planes that contain the matching directions having a small interplanar spacing misfit (f_d). Such planes are termed as matching planes. If these requirements are fulfilled, a favorable OR between the two phases can be constructed.

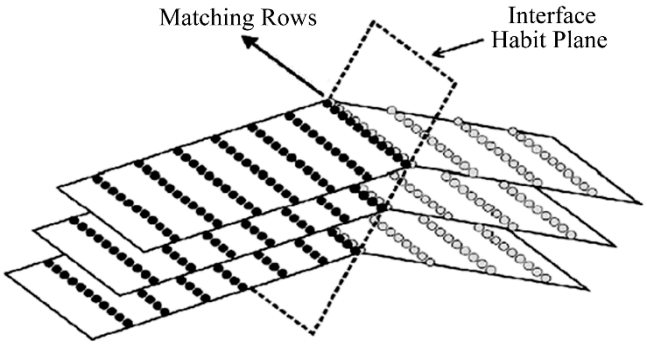

Figure 9. Schematic illustration of the interface formed through the edge-to-edge matching manner, reproduced from Reference [66], with permission of Elsevier, 2009.

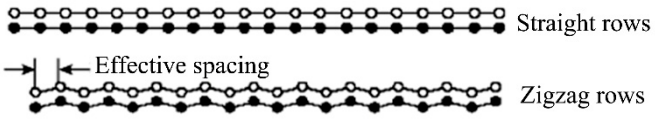

Figure 10. Schematic illustration of the two types of matching directions, reproduced from Reference [64], with permission of Elsevier, 2005.

Based on the identification of the CP (or nearly CP) rows and the CP (or nearly CP) planes, the interatomic spacing misfit (f_r) along the matching directions and the interplanar spacing mismatch (f_d) of the matching planes between the two phases can be calculated using the following equations [65]:

$$f_r = \frac{|r_M - r_P|}{r_P} \quad (4)$$

$$f_d = \frac{|d_M - d_P|}{d_P} \quad (5)$$

where r_M and r_P are the interatomic spacing along the matching directions, and d_M and d_P are the interplanar spacing of the matching planes between the matrix phase and the precipitate particle, respectively.

The empirical criteria of the E2EM model is that the values of f_r and f_d are both less than 10% [60].

Compared with the lattice disregistry theory, the E2EM model can not only estimate the atomic matching between two phases, but also predict the favorable ORs based on the lattice parameters and the positions of the atoms in the two phases. For systems with a simple crystal structure, the disregistry model and the E2EM model may give the same results. However, for systems with complicated crystal structure, the E2EM model has an advantage that it more accurately examines the actual matching between atoms. In addition, the E2EM model emphasizes CP or nearly CP planes/directions. This overcomes the problem of how to specify the low-index planes associated with

the lattice disregistry model. Since 2005 [78,79], although the E2EM model has been successfully used to understand the grain refinement mechanism and develop new grain refiners in Al, Mg, and their alloys [80,87–89], and cast Zn and Zn alloys [90,91], its application to grain refinement of steels is very limited. Most recently, Li et al. [92] conducted a comprehensive crystallographic study on the grain refinement efficiency of NbO, CeS, TiN, Ce_2O_3, and TiC for δ-ferrite using the edge-to-edge matching (E2EM) model. By calculating the misfit (f_r) values along the CP directions and mismatch (f_d) values between CP planes, it was predicted that NbO, CeS, TiN, Ce_2O_3, and TiC can all effectively refine the grains of δ-ferrite. According to the calculated values of f_r and f_d, the grain refining efficiency of these five compounds is ranked in the sequence of NbO > CeS > TiN > Ce_2O_3 > TiC, which agrees well with previously reported experimental results. Moreover, based on the E2EM calculations, the orientation relationships (ORs) between δ-ferrite and the five compounds have also been predicted. Some ORs were reported before, such as the Baker-Nutting OR between TiN and ferrite [93,94].

Li et al. [95] also identified LaB_6 as an effective grain refiner for ferritic steels based on the crystallographic study using the E2EM model. A 0.5 wt% addition of LaB_6 significantly refined the grains of the as-cast Fe-4Si alloy. However, due to the low thermodynamic stability, the externally added LaB_6 decomposed into La and B in the steel melt, which led to the formation of various compounds. Further investigations found that the grain refinement was attributed to the combined effects of the heterogeneous nucleation of δ-ferrite on La_2SO_2 and the solute effect of B. Crystallographic analysis based on the E2EM model indicated the excellence of atomic matching between δ-ferrite and the La_2SO_2. The predicted OR was also experimentally verified using the electron backscatter diffraction (EBSD) Kikuchi line diffraction technique.

Recently, Ji et al. [96] calculated the atomic matching and predicted the rough ORs between the Ce_2O_3/La_2O_3 oxides and the primary phases (δ-ferrite/γ-austenite) using the E2EM model. The calculations showed that both Ce_2O_3 and La_2O_3 can promote heterogeneous nucleation of δ-ferrite and γ-austenite during solidification and therefore refine the as-cast macrostructure and microstructure of the steels. However, the grain refining potency of Ce_2O_3 and La_2O_3 for δ-ferrite is higher than that for γ-austenite. For δ-ferrite, Ce_2O_3 is more efficient than La_2O_3. However, for γ-austenite, La_2O_3 is more efficient than Ce_2O_3.

3.3. Effects of La and Ce as Solutes

3.3.1. Solid Solution State of La and Ce in Steels

According to the Fe-La and Fe-Ce phase diagrams, the solid solubility of La and Ce in iron is almost zero even though they can completely dissolve in the Fe melt. Hence, during the solidification of steels, the majority of REs are rejected from the solid and segregates in the liquid at front of the solid-liquid interface. Such segregation may generate a constitutional supercooling zone that potentially leads to grain refinement of the δ-ferrite and/or γ-austenite through solute effect [60,97–103]. In addition, some studies indicated that the solid solubility of lanthanum and cerium in ferrite is not absolutely zero [104–106]. The measured value was around 10^{-6}–10^{-5} [105,106] orders of magnitude using the inductively coupled plasma mass spectrometry (ICP-MS) through the low-temperature electrolysis of the samples and fast separation of the rare earth compounds. As the RE atoms tend to segregate at grain boundaries, vacancies, and dislocations in engineering steels, a very small amount of such REs can be detected in the steels.

In spite of such low solid solubility of REs, it has attracted great interest and attention of researchers and engineers in order to understand the roles RE solutes in grain refinement of cast steels [23,47,51,52].

3.3.2. Solute Effect of Grain Refinement in Cast Metals

In addition to the heterogeneous nucleation, the solutes also play crucial roles in the grain refinement of cast alloys. It is generally accepted that the role of the solute is attributed to the solute segregation in the liquid phase ahead of the solid-liquid interface [97,98]. The main points are:

(1) the solute segregation can restrict the growth of the previously formed solid phase; (2) the solute segregation can generate a constitutional supercooling (C_S) zone in the liquid phase ahead of the solid-liquid interface, which provides additional driving force to facilitate the subsequently new nucleation within the C_S zone; and (3) the newly formed grains restrict the further growth of the previously formed grains. The efficiency of grain refinement by the solute can be quantitatively expressed by the growth restriction factor (GRF or Q-value) [99–102]. The Q-value represents the establishing rate of the C_S zone. The solute with higher Q value corresponds to high grain refinement efficiency. In a binary system, the Q-value can be simply expressed as [101]:

$$Q = mC_0(k - 1) \tag{6}$$

where m is the slope of the liquidus in the binary phase diagram, C_0 is the content of the solute element in the alloy (mass%), k is the equilibrium partition coefficient of the solute element, and the unit of Q is K.

For the multicomponent systems, the calculation of Q is far more complex. A rigorous approach to calculate Q in multicomponent alloys based on the thermodynamics of the alloy phase equilibria was presented by Schmid-Fetzer and Kozlov [103], which was expressed using Equation (7) as follows:

$$Q = \left(\frac{\partial(\Delta T_{cs})}{\partial f_s}\right)_{f_s \to 0} \tag{7}$$

where ΔT_{cs} was the constitutional supercooling and f_s was the fraction of solid. However, it is still unknown whether the Equation (7) can be directly applied to the system of Fe-C-M-RE (M represents different alloying elements) in which the solid solution content of RE is extremely small. In the past few years, the concept of growth restriction factor has been widely used in study of the grain refinement of cast light metals and alloys [60,107] and cast zinc and Zn alloys [99,108–110].

Hu et al. [111] reported that the addition of Ce decreased the secondary dendrite arm spacing, enlarged the proportion of equiaxial grains, and refined the equiaxed grains of a low-sulfur 16Mn steel. It was considered that the increase in the equilibrium partition coefficients of carbon and manganese by Ce was responsible for the grain refinement. In addition, Hu and co-workers [112] investigated the influence of Ce on the morphology of austenite in a high-Mn steel using the directional solidification technique. It was found that with an increase in Ce content, the cellular structure gradually changed to dendrites and the columnar region was narrowed. It was considered that the solute Ce increases the partition coefficient of Mn. Zhong et al. [113] reported similar results showing that Ce slightly dissolved in austenite, leading to the increase in the equilibrium partition coefficient of Mn and decrease for Si. In a weather-resistant steel, Guo and co-workers [114–116] detected the enrichment of REs ahead of the solid-liquid interface, which corresponded to the increase in the non-equilibrium partition coefficient of various solute elements. According to Equation (6), for binary systems, when the partition coefficient of solute (k) is less than 1, the smaller the k is, the larger the value of Q is, and vice versa. For multicomponent systems, such as steels, the calculation of Q is complicated and the effect of REs on the value of Q needs to be studied in depth.

Ji et al. [117] calculated the Q values of a few solutes (Ti, Zr, Ce, La, Nb, and V) in the Fe-X binary alloy systems based on the calculated binary phase diagrams using the phase diagram module of the FactSage software system. The calculated Q values were ranked in the order of Ti > Zr > Ce > La > Nb > V. This result may explain the good grain refining efficiency of Ti and Zr used in steels. It is worth conducting further experimental work to verify the prediction.

4. Summary

(1) The addition of lanthanum or/and cerium in steel leads to the increase in the proportion of equiaxed crystal zone or the reduction in the average grain size or both. Commonly, it is considered that the structure refinement is attributed mainly to the heterogeneous nucleation of

high melting-point RE oxides, oxysulfides, and sulfides for δ-ferrite or γ-austenite, and possibly to the solute effects of lanthanum or/and cerium.

(2) The grain refining efficiency by additions of lanthanum or/and cerium varies in different steels. Furthermore, it is not clear for which phase, δ-ferrite or γ-austenite, the refining effect of REs is more efficient.

(3) The formation sequence of RE-containing inclusions in molten steel is RE oxides > RE oxysulfides > RE sulfides. The typical oxide is RE_2O_3. The oxysulfide is an intermediate product during the transition from deoxygenation to desulfuration by cerium and lanthanum. The variety and distribution of the RE oxysulfides rely on the contents of oxygen and sulfur and the condensate depression of the molten steel. The RE_2O_2S commonly forms. The type of RE sulfides is related to the ratio of RE content to S content, the value of [RE]/[S], in the molten steel. Typical sulfides are RE_2S_3, RE_3S_4, and RES.

(4) To evaluate the grain refining efficiency, although the two-dimensional disregistry model is widely used, the E2EM model is considered as a more accurate model, particularly for more complicated systems, because there is lack of clear criteria for selecting the low index planes in the two-dimensional disregistry model, which may cause inconsistent results.

(5) Compared with other models/theories evaluating the heterogeneous nucleation potency, the E2EM model is the most available and powerful tool for understanding the efficiency of nucleants and discovering effective grain refiners from the point of crystallographic view. The effects of solute on grain refinement are described mainly using the growth restriction factor (Q value) theory. Although the study on the Q value theory of ternary or multivariate iron-base alloy system with addition of rare earth has not been reported, the theory has been widely accepted for its successful explanation of the grain refinement of cast light metals and alloys. The E2EM model and the growth restriction theory can provide theoretical basis and feasible approaches to clarify previous inconsistence, leading to full understanding of the structural refinement mechanism of as-cast steels after adding REs.

Author Contributions: Y.J.: Writing—Original draft preparation, funding acquisition; M.-X.Z.: Writing—Review and editing; H.R.: Writing—Review and editing and supervision.

Funding: This work was financially supported by the National Natural Science Foundation of China (grant No. 51761034 and No. 51261018) and the Natural Science Foundation of Inner Mongolia in China (grant No. 2017MS0512).

Conflicts of Interest: The authors declare no conflict of interest.

References

1. Lan, P.; Song, L.; Du, C.; Zhang, J. Analysis of solidification microstructure and hot ductility of Fe-22Mn-0.7C TWIP steel. *Mater. Sci. Technol.* **2014**, *30*, 1297–1304. [CrossRef]
2. Zhuang, C.; Liu, J.; Mi, Z.; Jiang, H.; Tang, D.; Wang, G. Non-metallic inclusions in TWIP steel. *Steel Res. Int.* **2014**, *85*, 1432–1439. [CrossRef]
3. Chen, G.J.; Zhang, Y.J.; Wang, E.G.; Yang, Y.S. Industrial analysis of grain refinement under pulsed magnetic field during superalloy solidification. *Met. Funct. Mater.* **2014**, *21*, 29–33.
4. Li, Y.F.; Wen, G.H.; Tang, P.; Li, J.Q.; Xiang, C.L. Effect of slab subsurface microstructure evolution on transverse cracking of microalloyed steel during continuous casting. *J. Iron Steel Res. Int.* **2014**, *21*, 737–744. [CrossRef]
5. Irving, W.R. *Continous Casting of Steel*; Institute of Materials: London, UK, 1993; ISBN 9781907625381.
6. Buchmayr, B. Thermomechanical treatment of steels—A real disruptive technology since decades. *Steel Res. Int.* **2017**, *88*. [CrossRef]
7. Nishioka, K.; Ichikawa, K. Progress in thermomechanical control of steel plates and their commercialization. *Sci. Technol. Adv. Mater.* **2012**, *13*. [CrossRef]
8. Jin, W.Z.; Zhang, W.; Li, T.J.; Yin, G.M. Study of the grain refinement technology by electromagnetic stirring for IN100 superalloy vacuum investment casting. *Adv. Mater. Res.* **2011**, *189–193*, 3789–3794. [CrossRef]

9. Xu, Y.; Wang, E.G.; Li, Z.; Deng, A.Y. Effects of vertical electromagnetic stirring on grain refinement and macrosegregation control of bearing steel billet in continuous casting. *J. Iron Steel Res. Int.* **2017**, *24*, 83–489. [CrossRef]
10. Tzavaras, A.A.; Brody, H.D. Electromagnetic stirring and continuous casting—Achievements, problems, and goals. *JOM* **1984**, *36*, 31–37. [CrossRef]
11. Bridge, M.R.; Rogers, G.D. Structural effects and band segregate formation during the electromagnetic stirring of strand-cast steel. *Metall. Trans. B* **1984**, *15*, 581–589. [CrossRef]
12. Riestra, M.; Ghassemali, E.; Bogdanoff, T.; Seifeddine, S. Interactive effects of grain refinement, eutectic modification and solidification rate on tensile properties of Al-10SI alloy. *Mater. Sci. Eng. A* **2017**, *703*, 270–279. [CrossRef]
13. Ali, Y.; You, G.; Pan, F.; Zhang, M.X. Grain coarsening of cast magnesium alloys at high cooling rate: A new observation. *Metall. Mater. Trans. A* **2017**, *48*, 474–481. [CrossRef]
14. Quested, T.E. Understanding mechanisms of grain refinement of aluminium alloys by inoculation. *Met. Sci. J.* **2004**, *20*, 1357–1369. [CrossRef]
15. Lu, L.; Dahle, A.K.; Stjohn, D.H. Heterogeneous nucleation of Mg-Al alloys. *Scr. Mater.* **2006**, *54*, 2197–2201. [CrossRef]
16. Bramfitt, B.L. The effect of carbide and nitride additions on the heterogeneous nucleation behavior of liquid iron. *Metall. Trans.* **1970**, *1*, 1987–1995. [CrossRef]
17. Nakajima, K.; Hasegawa, H.; Khumkoa, S.; Mizoguchi, S. Effect of a catalyst on heterogeneous nucleation in pure and Fe-Ni alloys. *Metall. Mater. Trans. B* **2003**, *34*, 539–547. [CrossRef]
18. Ohno, M.; Matsuura, K. Refinement of as-cast austenite microstructure in S45C steel by titanium addition. *ISIJ Int.* **2008**, *48*, 1373–1379. [CrossRef]
19. Tuttle, R. Examination of steel castings for potential nucleation phases. *Int. J. Metalcast.* **2010**, *4*, 17–25. [CrossRef]
20. Suito, H.; Ohta, H.; Morioka, S. Refinement of solidification microstructure and austenite grain by fine inclusion particles. *Trans. Iron Steel Inst. Jpn.* **2006**, *46*, 840–846. [CrossRef]
21. Nuri, Y.; Ohashi, T.; Hiromoto, T.; Kitamura, O. Solidification microstructure of ingots and continuously cast slabs treated with rare earth metals. *Trans. Iron Steel Inst. Jpn.* **1982**, *22*, 399–407. [CrossRef]
22. Xie, J.P.; Wang, A.Q.; Wang, W.Y.; Li, J.W.; Li, L.L. Effect of rare earths on toughness of 31Mn2SiRE wear-resistance cast steel. *J. Rare Earths* **2006**, *24*, 401–404.
23. Guo, M.; Suito, H. Influence of dissolved cerium and primary inclusion particles of Ce_2O_3 and CeS on solidification behavior of Fe-0.20mass%C-0.02mass%P alloy. *Trans. Iron Steel Inst. Jpn.* **1999**, *39*, 722–729. [CrossRef]
24. Guo, M.; Suito, H. Dispersion of primary inclusions of Ce_2O_3 and CeS in Fe-0.20mass%C-0.02mass%P alloy. *ISIJ Int.* **1999**, *39*, 678–868. [CrossRef]
25. Tuttle, R.B. Experimental grain refiners for carbon steels. *Int. J. Metalcast.* **2016**, *10*, 1–11. [CrossRef]
26. Casper, V.D.E.; Øystein, G.; Fredrik, H.; Leiv, K.; Gabriella, T. Progress in the development and use of grain refiner based on cerium sulfide or titanium compound for carbon steel. *ISIJ Int.* **2009**, *49*, 1046–1050.
27. Dadkhah, H. Microstructure of cast ultrahigh carbon steel (UHCS) modified via Fe-Si-Mg-Ca-RE. *Trans. Indian Inst. Met.* **2014**, *67*, 1001–1004. [CrossRef]
28. Wang, L.; Tan, Q.; Li, N.; Qin, Z.; Qiu, S.; Gan, Y. Research progress on rare earth application technology in non-oriented electrical steels. *J. Chin. Soc. Rare Earths* **2014**, *32*, 513–533.
29. Li, H.Z.; Liu, H.T.; Wang, X.L.; Cao, G.M.; Li, C.G.; Liu, Z.Y.; Wang, G.D. Effect of cerium on the as-cast microstructure and tensile ductility of the twin-roll casting Fe-6.5 wt% Si alloy. *Mater. Lett.* **2016**, *165*, 5–8. [CrossRef]
30. Gao, J.; Fu, P.; Liu, H.; Li, D. Effects of rare earth on the microstructure and impact toughness of H13 steel. *Metals* **2015**, *5*, 383–394. [CrossRef]
31. Bartlett, L.N.; Avila, B.R. Grain refinement in lightweight advanced high-strength steel castings. *Int. J. Metalcast.* **2016**, *10*, 401–420. [CrossRef]
32. Pan, F.; Zhang, J.; Chen, H.L.; Su, Y.H.; Kuo, C.L.; Su, Y.H.; Chen, S.H.; Lin, K.J.; Hsieh, P.H.; Hwang, W.S. Effects of rare earth metals on steel microstructures. *Materials* **2017**, *9*, 417. [CrossRef] [PubMed]
33. Smirnov, L.A.; Rovnushkin, V.A.; Oryshchenko, A.S.; Kalinin, G.Y.; Milyuts, V.G. Modification of steel and alloys with rare-earth elements-Part 1. *Metallurgist* **2016**, *59*, 1053–1061. [CrossRef]

34. Smirnov, L.A.; Rovnushkin, V.A.; Oryshchenko, A.S.; Kalinin, G.Y.; Milyuts, V.G. Modification of steel and alloys with rare-earth elements-Part 2. *Metallurgist* **2016**, *60*, 38–46. [CrossRef]
35. Jeon, S.H.; Hur, D.H.; Kim, H.J.; Park, Y.S. Effect of Ce addition on the precipitation of deleterious phases and the associated intergranular corrosion resistance of 27Cr-7Ni hyper duplex stainless steels. *Corros. Sci.* **2015**, *90*, 313–322. [CrossRef]
36. Hamidzadeh, M.A.; Meratian, M.; Saatchi, A. Effect of cerium and lanthanum on the microstructure and mechanical properties of AISI D2 tool steel. *Mater. Sci. Eng. A* **2013**, *571*, 193–198. [CrossRef]
37. Fang, Q.; Song, W.Z.; Sun, W.; Jin, Z.L.; Ren, H.P. Effect of rare earth (La) on dynamic softening and precipitation of low carbon high niobium steel. *Adv. Mater. Res.* **2012**, *509*, 64–67. [CrossRef]
38. Wen, Z.; Yi, D.Q.; Wang, B.; Shi, S.Q.; Zhang, Y.K. Effect of rare earths on the recrystallization behavior of T91 heatresistant steel. *J. Univ. Sci. Technol. Beijing* **2013**, *35*, 1000–1006.
39. Petryna, D.Y.; Kozak, O.L.; Shulyar, B.R.; Hredil, M.I. Influence of alloying by rare-earth metals on the mechanical properties of 17g1s pipe steel. *Mater. Sci.* **2013**, *48*, 575–581. [CrossRef]
40. Zhao, Y.; Wang, J.; Zhou, S.; Wang, X. Effect of rare earth addition on microstructure and mechanical properties of a Fe-15Mn-1.5Al-0.6C TWIP steel. *Mater. Sci. Eng. A* **2014**, *608*, 106–113. [CrossRef]
41. Wan, Y.; Chen, W.Q.; Wu, S.J. Effect of lanthanum content on microstructure and magnetic properties of non-oriented electrical steels. *J. Rare Earths* **2013**, *31*, 727–733. [CrossRef]
42. Yang, J.C.; Yang, C.Q. Effects of cerium on hot deformation behavior of IF steel. *J. Chin. Soc. Rare Earths* **2014**, *32*, 346–353.
43. Haakonsen, F.; Solberg, J.K.; Klevan, O.S.; Eijk, C.V.D. Grain refinement of austenitic manganese steels. *AISTech 2011 Proceedings* **2011**, *2*, 763–771.
44. Qiu, D.; Zhang, M.-X.; Taylor, J.A.; Fu, H.-M.; Kelly, P.M. A novel approach to the mechanism for the grain refining effect of melt superheating of Mg-Al alloys. *Acta Mater.* **2007**, *55*, 1863–1871. [CrossRef]
45. Zhang, M.X.; Kelly, P.M.; Easton, M.A.; Taylor, J.A. Crystallographic study of grain refinement in aluminum alloys using the edge-to-edge matching model. *Acta Mater.* **2005**, *53*, 1427–1438. [CrossRef]
46. Zhang, H.; Cui, W.F.; Wang, J.J.; Liu, C.M. Effect of Ce addition on hot ductility of 00Cr17 high-purity ferrite stainless steel. *Trans. Mater. Heat Treat.* **2011**, *32*, 61–66.
47. Xu, J.; Qi, G.P.; Zhu, J.X.; Xu, B.; Zhang, K.; Wang, L.M. Effects of RE on solidification structure and sheet metal formability of ferrite stainless steels (430). *J. Chin. Soc. Rare Earths* **2006**, *24*, 486–489.
48. Tuttle, R. Effect of rare earth additions on grain refinement on plain carbon steels. *Int. J. Metalcast.* **2012**, *6*, 51–65. [CrossRef]
49. Tuttle, R. Understanding the mechanism of grain refinement in plain carbon steels. *Int. J. Metalcast.* **2013**, *7*, 7–16. [CrossRef]
50. Tuttle, R.; Song, K. Characterization of rare earth inclusions from cast 1010 steel. *Int. J. Metalcast.* **2015**, *9*, 23–31. [CrossRef]
51. Wang, A.-Q.; Li, M.; Ma, D.-Q.; Wu, Q.-J.; Xie, J.-P. Effect of Lanthanum on microstructures and properties of ASTM A216 steel. *Kem. Ind.* **2016**, *65*, 11–16. [CrossRef]
52. Li, H.; Mclean, A.; Rutter, J.W.; Sommerville, I.D. Influence of rare earth metals on the nucleation and solidification behavior of iron and 1045 steel. *Metall. Mater. Trans. B* **1988**, *19*, 383–395. [CrossRef]
53. Wang, L.M.; Lin, Q.; Yue, L.J.; Liu, L.; Guo, F.; Wang, F.M. Study of application of rare earth elements in advanced low alloy steels. *J. Alloys Compd.* **2008**, *451*, 534–537. [CrossRef]
54. Zhu, Y.G.; Liu, Y.; Liu, Z.L.; Liu, W.D. Analysis of valence electron structure of RE in solid solution in medium and low carbon steel. *J. Rare Earths* **2004**, *22*, 282–287.
55. Lin, Q.; Song, B.; Guo, X.M.; Zhang, M. Effects of RE on microalloying in steel and application prospects. *Chin. Rare Earths* **2001**, *22*, 31–36.
56. Guo, F.; Lin, Q. Existing forms of rare earth element La in purity steel. *J. Chin. Soc. Rare Earths* **2006**, *24*, 501–504.
57. Pan, F.; Su, Y.H.; Augusto, J.; Hwang, W.S.; Chen, H.L. Optical inclusion transformation with different amount of cerium addition during solidification of ss400 steel. *Opt. Quantum Electron.* **2016**, *48*, 536. [CrossRef]
58. Li, Y.-D.; Liu, C.J.; Li, C.-L.; Jiang, M.F. A coupled thermodynamic model for prediction of inclusions precipitation during solidification of heat-resistant steel containing cerium. *J. Iron Steel Res.* **2015**, *22*, 457–463. [CrossRef]

59. Song, M.M.; Song, B.; Xin, W.B.; Sun, G.L.; Song, G.Y.; Hu, C.L. Effects of rare earth addition on microstructure of C-Mn steel. *Ironmak. Steelmak.* **2015**, *42*, 594–599. [CrossRef]
60. Ali, Y.; Qiu, D.; Jiang, B.; Pan, F.; Zhang, M.X. Current research progress in grain refinement of cast magnesium alloys: A review article. *J. Alloys Compd.* **2015**, *619*, 639–651. [CrossRef]
61. Turnbull, D.; Vonnegut, B. Nucleation catalysis. *Ind. Eng. Chem.* **1952**, *44*, 1292–1298. [CrossRef]
62. Tiller, W.A.; Takahashi, T. The electrostatic contribution in heterogeneous nucleation theory: Pure liquids. *Acta Metall.* **1969**, *17*, 483–496. [CrossRef]
63. Yu, R.H. Empirical electron theory of solids and molecules. *Chin. Sci. Bull.* **1978**, *23*, 217–224.
64. Zhang, M.-X.; Kelly, P.M. Edge-to-edge matching model for predicting orientation relationships and habit planes—The improvements. *Scr. Mater.* **2005**, *52*, 963–968. [CrossRef]
65. Kelly, P.M.; Zhang, M.-X. Edge-to-Edge Matching—A New approach to the morphology and crystallography of precipitates. *Mater. Forum* **1999**, *23*, 41–62.
66. Zhang, M.X.; Kelly, P.M. Crystallographic features of phase transformations in solids. *Prog. Mater. Sci.* **2009**, *54*, 1101–1170. [CrossRef]
67. Yi, D.; Zhang, Z.; Fu, H.; Yang, C.; Ma, S.; Li, Y. A study on the microstructures and toughness of Fe-B cast alloy containing rare earth. *J. Mater. Eng. Perform.* **2015**, *24*, 626–634. [CrossRef]
68. Hao, F.F.; Liao, B.; Li, D.; Liu, L.G.; Dan, T.; Ren, X.J.; Yang, Q.X. Effects of rare earth oxide on hardfacing metal microstructure of medium carbon steel and its refinement mechanism. *J. Rare Earths* **2011**, *29*, 609–613. [CrossRef]
69. Yang, J.; Hao, F.F.; Li, D.; Zhou, Y.F.; Ren, X.J.; Yang, Y.L.; Yang, Q.X. Effect of RE oxide on growth dynamics of primary austenite grain in hardfacing layer of medium-high carbon steel. *J. Rare Earths* **2012**, *30*, 814–819. [CrossRef]
70. Pan, N.; Song, B.; Zhai, Q.J.; Wen, B. Effect of lattice disregistry on the heterogeneous nucleation catalysis of liquid steel. *J. Univ. Sci. Technol. Beijing* **2010**, *32*, 179–182.
71. Tian, Y.; Wu, H.; Guo, J.; Li, F. Effect of RE inclusions on heterogeneous nucleation of primary austenite in Fe-C alloys. *J. Chin. Rare Earth Soc.* **1988**, *6*, 45–48.
72. Liao, B.; Gao, Z.S. Study on heterogeneous nucleation of primary austenite in semi-steel—The effect RE inclusion and common oxide in semi-steel. *Trans. Met. Heat Treat.* **1991**, *12*, 60–64.
73. Yu, Y.; Zhang, S.; Li, H.; Wang, S. Effects of rare earth lanthanum on the solidification structure and hot ductility of Fe-43Ni expansion alloy. *High Temp. Mater. Process.* **2018**, *37*, 261–269. [CrossRef]
74. Yang, Q.X.; Ren, X.J.; Liao, B.; Yao, M. Discussion of RE Inclusions as Heterogeneous Nuclei of Primary Austenite in Hardfacing Metals of Medium-High Carbon Steels. *J. Rare Earths* **1999**, *17*, 293–297.
75. Liang, G.F.; Xu, Z.M.; Qu, D.K.; Song, C.J.; Liu, X.Y.; Li, J.G. The valence electron criterion on heterogeneous nucleus catalysis during non-equilibrium solidification of austenite steel. *J. Shanghai Jiaotong Univ.* **2005**, *39*, 1073–1076, 1081.
76. Liang, G.; Song, C.; Liu, X.; Xu, Z.; Li, J. Valence electron model on heterogeneous nucleation of Au liquid and nuclei catalysis. *Rare Met. Mater. Eng.* **2005**, *34*, 1558–1661.
77. Pan, N.; Song, B.; Zhai, Q. Catalysis on heterogeneous nucleation of solid compounds in liquid steel. *Acta Metall. Sin.* **2009**, *45*, 1441–1445.
78. Zhang, M.-X.; Kelly, P.M.; Qian, M.; Taylor, J.A. Crystallography of grain refinement in Mg-Al based alloys. *Acta Mater.* **2005**, *53*, 3261–3270. [CrossRef]
79. Zhang, M.X.; Kelly, P.M. Understanding the crystallography of the eutectoid microstructure in a Zn-Al alloy using the edge-to-edge matching model. *Scr. Mater.* **2006**, *55*, 577–580. [CrossRef]
80. Ali, Y.; Qiu, D.; Jiang, B.; Pan, F.S.; Zhang, M.-X. The influence of CaO addition on grain refinement of cast magnesium alloys. *Scr. Mater.* **2016**, *114*, 103–107. [CrossRef]
81. Wang, F.; Qiu, D.; Liu, Z.-L.; Taylor, J.A.; Easton, M.A.; Zhang, M.-X. Crystallographic study of grain refinement of Al by Nb addition. *J. Appl. Crystallogr.* **2014**, *47*, 770–779. [CrossRef]
82. Hall, M.G.; Aaronson, H.I.; Kinsma, K.R. The structure of nearly coherent fcc: Bcc boundaries in a Cu-Cr alloy. *Surf. Sci.* **1972**, *31*, 257–274. [CrossRef]
83. Rigsbee, J.M.; Aaronson, H.I. A computer modeling study of partially coherent f.c.c.: b.c.c. boundaries. *Acta Metall.* **1979**, *27*, 351–363. [CrossRef]
84. Dahmen, U. Orientation relationships in precipitation systems. *Acta Metall.* **1982**, *30*, 63–73. [CrossRef]

85. Luo, C.P.; Weatherly, G.C. The invariant line and precipitation in a Ni-45 wt% Cr alloy. *Acta Metall.* **1987**, *35*, 1963–1972. [CrossRef]
86. Bollmann, W. Crystal defects and crystalline interfaces. *Trans. Am. Microsc. Soc.* **1970**, *91*, 247.
87. Qiu, D.; Zhang, M.X.; Kelly, P.M. Crystallography of heterogeneous nucleation of Mg grain on Al_2Y nucleation particles in an Mg-10 wt% Y alloy. *Scr. Mater.* **2009**, *61*, 312–315. [CrossRef]
88. Qiu, D.; Zhang, M.X. The nucleation crystallography and wettability of Mg grains on active Al_2Y inoculants in an Mg-10 wt % Y Alloy. *J. Alloys Compd.* **2014**, *586*, 39–44. [CrossRef]
89. Wang, F.; Qiu, D.; Liu, Z.-L.; Taylor, J.A.; Easton, M.A.; Zhang, M.-X. The grain refinement mechanism of cast aluminium by zirconium. *Acta Mater.* **2013**, *61*, 5636–5645. [CrossRef]
90. Liu, Z.; Qiu, D.; Wang, F.; Taylor, J.A.; Zhang, M. The grain refining mechanism of cast zinc through silver inoculation. *Acta Mater.* **2014**, *79*, 315–326. [CrossRef]
91. Liu, Z.; Qiu, D.; Wang, F.; Taylor, J.A.; Zhang, M. Crystallography of grain refinement in cast zinc-copper alloys. *J. Appl. Crystallogr.* **2015**, *48*, 890–900. [CrossRef]
92. Li, M.; Li, J.; Qiu, D.; Zheng, Q.; Wang, G.; Zhang, M. Crystallographic study of grain refinement in low and medium carbon steels. *Philos. Mag.* **2016**, *96*, 1–23. [CrossRef]
93. Gregg, J.M.; Bhadeshia, H.K.D.H. Solid-state nucleation of acicular ferrite on minerals added to molten steel. *Acta Mater.* **1997**, *45*, 739–748. [CrossRef]
94. Mills, A.R.; Thewlis, G.; Whiteman, J.A. Nature of inclusions in steel weld metals and their influence. *Met. Sci. J.* **2013**, *3*, 1051–1061.
95. Li, M.; Li, J.M.; Zheng, Q.; Qiu, D.; Wang, G.; Zhang, M.-X. A New Grain Refiner for Ferritic Steels. *Metall. Mater. Trans. B* **2017**, *48*, 1–11. [CrossRef]
96. Ji, Y.; Kang, L.; Song, Y.; Qu, W.; Ren, H. Crystallographic calculation about heterogeneous nucleation potency of RE_2O_3 in Liquid Steel. *Rare Met. Mater. Eng.* **2017**, *46*, 2889–2894.
97. Stjohn, D.H.; Qian, M.; Easton, M.A.; Cao, P. The Interdependence Theory: The relationship between grain formation and nucleant selection. *Acta Mater.* **2011**, *59*, 4907–4921. [CrossRef]
98. Stjohn, D.H.; Easton, M.A.; Qian, M.; Taylor, J.A. Grain Refinement of Magnesium Alloys: A review of recent research, theoretical developments, and their application. *Metall. Mater. Trans. A* **2013**, *44*, 2935–2949. [CrossRef]
99. Easton, M.A.; Qian, M.; Prasad, A.; Stjohn, D.H. Recent advances in grain refinement of light metals and alloys. *Curr. Opin. Solid State Mater. Sci.* **2016**, *20*, 13–24. [CrossRef]
100. Qian, M.; Cao, P.; Easton, M.A.; Mcdonald, S.D.; Stjohn, D.H. An analytical model for constitutional supercooling-driven grain formation and grain size prediction. *Acta Mater.* **2010**, *58*, 3262–3270. [CrossRef]
101. Easton, M.; Stjohn, D. Grain refinement of aluminum alloys: Part I. the nucleant and solute paradigms—A review of the literature. *Metall. Mater. Trans. A* **1999**, *30*, 1613–1623. [CrossRef]
102. Stjohn, D.H.; Ma, Q.; Easton, M.A.; Cao, P.; Hildebrand, Z. Grain refinement of magnesium alloys. *Metall. Mater. Trans. A* **2005**, *36*, 1669–1679. [CrossRef]
103. Schmid-Fetzer, R.; Kozlov, A. Thermodynamic aspects of grain growth restriction in multicomponent alloy solidification. *Acta Mater.* **2011**, *59*, 6133–6144. [CrossRef]
104. Liu, Y.H.; Lin, Q.; Ye, W.; Chen, N.; Guo, Y.; Chen, Z.Q.; Zhu, Q.H. Behavior of rare earths in ultra-low-sulfur microalloyed steel. *J. Rare Earths* **1999**, *17*, 207–212.
105. Yue, L.J.; Wang, L.L.; Wang, L.M. Influence of rare earth element on the mechanical properties of clean weathering steel. *J. Rare Earths* **2014**, *35*, 20–26.
106. Ji, Y.; Ren, H.; Liu, X.; Hou, J.; Jin, Z. Effect of rare earth on super-cooled austenite transformation of 20MnCrNi2Mo wear-resistant cast steel and its mechanism. *Rare Met. Mater. Eng.* **2017**, *46*, 997–1102.
107. Wang, F.; Liu, Z.-L.; Qiu, D.; Taylor, J.A.; Easton, M.A.; Zhang, M.-X. The influence of the effect of solute on the thermodynamic driving force on grain refinement of Al alloys. *Metall. Mater. Trans. A* **2015**, *46*, 505–515. [CrossRef]
108. Liu, Z.; Li, R.; Jiang, R.; Li, X.; Zhang, M. Effects of Al addition on the structure and mechanical properties of Zn alloys. *J. Alloys Compd.* **2016**, *687*, 885–892. [CrossRef]
109. Liu, Z.L.; Wang, F.; Qiu, D.; Taylor, J.A.; Zhang, M.X. The effect of solute elements on the grain refinement of cast Zn. *Metall. Mater. Trans. A* **2013**, *44*, 4025–4030. [CrossRef]
110. Liu, Z.L.; Qiu, D.; Wang, F.; Taylor, J.A.; Zhang, M.X. Grain refinement of cast zinc through magnesium inoculation: Characterisation and mechanism. *Mater. Charact.* **2015**, *106*, 1–10. [CrossRef]

111. Hu, H.Q.; Zhong, X.Y.; Han, Q.Y. Effect of Ce on solidification structure of low sulphur 16Mn steel. *Acta Metall. Sin.* **1987**, *23*, 176–181.
112. Hu, H.Q.; Zhong, X.Y.; Li, H. Influence of Ce on crystal morphology of austensite and dendritic segregation of Mn in high-Mn steel. *Acta Metall.* **1984**, *20*, 247–254.
113. Zhong, X.Y.; Hu, H.Q.; Liu, C.M. The measurement of cerium equilibrium partition coefficient K_0 and influence of cerium on value of manganese and silicon K_0 in high manganese steel. *J. Univ. Sci. Technol. Beijing* **1984**, 16–22.
114. Guo, H.H.; Song, B.; Mao, J.H.; Zhao, P. Effect of rare earth elements on macrosegregation in weather-resisting steel. *J. Univ. Sci. Technol. Beijing* **2010**, *32*, 44–49.
115. Guo, H.H.; Song, B.; Hou, L.S.; Mao, J.H.; Zhao, P. Effect of RE on phosphorus macrosegregation of weather-resisting steel. *Chin. Rare Earths* **2011**, *32*, 53–57.
116. Guo, H.H.; Song, B.; Hou, L.S.; Mao, J.H.; Zhao, P. Effects of RE on solute redistribution of weather-resisting steel. *J. Chin. Rare Earth Soc.* **2010**, *28*, 360–365.
117. Ji, Y.; Kang, L.; Li, C.; Song, Y.; Ren, H. Effect of rare-metal solute on refinement of solidification microstructure in Fe-X binary alloys. *Chin. J. Rare Met.* **2018**, *42*, 362–366.